Biological Conservation 257 (2021) 109086

Contents lists available at ScienceDirect

Biological Conservation

journal homepage: www.elsevier.com/locate/biocon

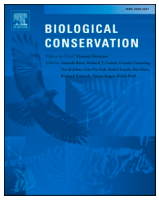

Effects of human-altered landscapes on a reintroduced ungulate: Patterns of habitat selection at the rangeland-wildland interface

Lacey F. Hughey [a,b,c,*], Kevin T. Shoemaker [d], Kelley M. Stewart [d], Douglas J. McCauley [a,e], J. Hall Cushman [d]

[a] Department of Ecology, Evolution and Marine Biology, University of California, Santa Barbara, CA 93106, USA
[b] Conservation Ecology Center, Smithsonian Conservation Biology Institute, National Zoological Park, Front Royal, VA 22630, USA
[c] Movement of Life, Conservation Commons, Smithsonian Institution, Washington, DC, 20013, USA
[d] Department of Natural Resources and Environmental Science, University of Nevada, Reno, NV 89557, USA
[e] Marine Science Institute, University of California, Santa Barbara, CA, 93106, USA

ARTICLE INFO

Keywords:
Habitat selection
Rangeland-wildland interface
Reintroduced ungulates
Resource selection
Satellite remote sensing-based animal detection
Tule elk

ABSTRACT

Successful species reintroductions require land managers to balance the goal of viable wildlife populations with potential risks to human enterprise. Such risks are particularly acute at the wildland-agriculture interface, where native and domestic species are likely to come into contact. In a national park in northern California, we combined insights from three lines of evidence – long-term visual surveys, short-term GPS telemetry, and satellite remote sensing-based animal detections – to characterize spatial overlap between reintroduced tule elk (*Cervus canadensis nannodes*) and domestic cattle and to estimate the importance of multiple environmental features as predictors of habitat selection by elk. Our results indicate that, at large spatial scales (i.e., home-range level), cattle were the primary driver of habitat selection, with the occurrence of elk being negatively associated with cattle across all seasons. In addition, elk consistently selected for grasslands on gentle, south-facing slopes that occurred at high elevation and close to ponds. NDVI was a seasonally important, positive predictor of habitat selection, with a marked reversal when this resource was concentrated inside of fenced cow pastures during the dry summer months. By contrast, a novel analysis of satellite-derived animal locations yielded no evidence of avoidance of cattle by elk (within pasture areas commonly used by elk), indicating that this population has acclimated to the presence of cattle through spatial partitioning of resources. Thus, this once-imperiled native ungulate exhibits patterns of habitat selection that reduce the potential for grazing conflicts with cattle, even in cases where access to forage is limited.

1. Introduction

Following centuries of megafaunal declines in North America, numerous restoration projects have aimed to return native populations of wildlife to their known historical ranges (Seddon et al., 2014). These efforts have produced notable conservation achievements, but also revealed a number of significant challenges associated with maintaining free-roaming wildlife populations in proximity to human-modified landscapes (Armstrong and Seddon, 2008). The growing literature on this topic suggests that such challenges are often amplified in agricultural landscapes, where reintroduced megafauna may come into contact with closely related domestic species (Hibert et al., 2010; Merkle et al., 2018; Proffitt et al., 2011). Given the documented potential for conflict (e.g., forage competition, behavioral exclusion, disease transmission) between livestock and reintroduced ungulates, much of this literature has focused on documenting the effects of interactions between these two groups.

Importantly, this research suggests that interactions between livestock and native ungulates are complex and can range from competition to facilitation, depending on the natural history of the system (Scasta et al., 2016; Schieltz and Rubenstein, 2016). For example, the ability to migrate is one of many factors that may reduce pressure on shared resources (at least seasonally) and contribute to an increased likelihood of sustained coexistence between wildlife and livestock. However, a reintroduced population that does not migrate, and thus remains in contact with livestock year-round, raises a suite of unanswered questions about

* Corresponding author at: Smithsonian Conservation Biology Institute, National Zoological Park, 1500 Remount Road, Front Royal, VA 22630, USA.
E-mail address: hugheyl@si.edu (L.F. Hughey).

https://doi.org/10.1016/j.biocon.2021.109086
Received 25 August 2020; Received in revised form 15 March 2021; Accepted 21 March 2021
Available online 10 April 2021

the ecological mechanisms that explain the coexistence of these two potentially competing populations. Likewise, the question of scale looms large when seeking explanations for observed ecological patterns, as processes observed at one scale may not persist when assessed from an alternative scale (Chave, 2013). As a result, clarifying both the mechanism and scale of an ecological pattern is critical to obtaining actionable conservation insights and accurately assessing the potential for conflict between reintroduced megafauna and domestic livestock.

The challenge with this approach, however, is that it requires detailed information on the simultaneous distributions of wildlife and livestock over large expanses of space and time- data which is notoriously difficult to acquire. Our study aims to address such limitations by presenting a novel application of emerging satellite remote sensing (SRS) technology to quantify species interactions and patterns of habitat selection at a rangeland-wildland interface in northern California. This unique study site afforded several strategic advantages for SRS-based research, including a moderately sized ($n = 93$), non-migratory population of reintroduced tule elk (*Cervus canadensis nannodes*), open landscapes with high visibility, and long-term datasets on the distribution of elk and cattle across the entire study area. When combined with SRS-derived animal locations, these datasets (e.g., GPS telemetry and visual surveys) yielded scale-dependent insights into the habitat selection processes that contribute to the persistence of a reintroduced ungulate in a cattle-dominated ecosystem.

Specifically, we used SRS-derived animal locations to produce a spatially explicit time series of livestock densities across the entire study area. We then used GPS telemetry and visual surveys to identify large-scale, seasonal patterns of resource selection by elk in response to this gradient of livestock densities. Finally, we applied the SRS-derived animal locations to a fine-scale investigation of the drivers of coexistence between elk and livestock across the system. By combining insights from multiple data streams, we revealed that coexistence between elk and cattle is maintained by a unique combination of avoidance (at large scales) and tolerance for proximity (at small scales). As such, this study yields new insights into the nature of interspecific interactions in this ecosystem, while providing a novel and replicable model for quantifying the dynamics of livestock-wildlife interactions in remote landscapes elsewhere.

2. Materials and methods

2.1. Study area

Our research was conducted in Point Reyes National Seashore, approximately 65 km northwest of San Francisco, California. The region experiences a Mediterranean climate, with moderate, rainy winters (mean temperature 10 °C, mean rainfall 17 cm) and cool, foggy summers with very little precipitation (mean temperature 14 °C, mean rainfall 14 cm; [dataset] "Western Regional Climate Center", 2020). The study site (hereafter, 'Drake's Beach') encompasses a 30 km^2 area comprised of fenced dairy cattle ranches (ca. 18 km^2, operated under lease agreements with the National Park Service) and adjacent wildlands that are not grazed by cattle (ca. 6.5 km^2; Fig. 1). Ranches are dominated by open coastal scrub (*Baccharis* spp. *and Lupinus arboreus*; 47% cover), barren sand dunes (16% cover), and highly disturbed active pastures (14% cover). Native grassland composes <7% of this habitat type. Wildlands are dominated by native grassland (53% cover), dune vegetation (*Lupinus chamissonis*, *Artemisia pycnocephala*, *Ammophila arenaria*; 21% cover), and open coastal scrub (*Baccharis* spp. *and Lupinus arboreus*; 7% cover). The relatively flat (elevation ranges from sea level to 112 m), open landscape is bisected by two paved roads that afford unobstructed views across 95% of the study area.

Fig. 1. Map of study area within Point Reyes National Seashore, CA. Elk home range represents a 95% autocorrelated kernel density estimate (Fleming and Calabrese, 2016) for all collared elk in the study area ($n = 8$, data collected from 2012 to 2017). Survey sites are shaded to indicate relative mean density of elk, darker shades indicate higher density.

2.2. Study species

Originally extirpated from the Point Reyes peninsula due to hunting and habitat loss, tule elk were absent from the study area for at least 100 years before a small group ($n = 28$) was reintroduced to a designated wilderness area in 1999 (Howell et al., 2002). Soon after reintroduction, several elk dispersed to the current study area and established a new population that numbered 93 animals as of 2016 (Bernot and Press, 2018). This group is known as the 'Drake's Beach Herd' and inhabits a home range of ca. 6 km^2 within the Pastoral Zone of Point Reyes National Seashore (Fig. 1). Hunting is prohibited throughout the study area and previous research suggests that predation is not a significant source of mortality for elk in this ecosystem (Cobb, 2010; Thomas and Toweill, 2002).

2.3. Elk activity and habitat characteristics

We used three complementary datasets to assess elk activity and selection of habitats at the following scales: (1) Home range scale (visual surveys and GPS telemetry) and (2) Pasture scale (satellite remote sensing-based animal detections). The use of multiple datasets allowed us to make robust conclusions about patterns observed at the home range scale and derive new insights about the mechanisms that maintain coexistence between elk and cattle in this system. For all analyses, we partitioned elk activity into four biologically relevant seasons: wet season (November–April), parturition (May–June), summer (July–August), and mating season (September–October).

2.3.1. Visual surveys

All surveys ($n = 589$) were performed between September 2010 and October 2017 (mean = 73 surveys/year) by the same park biologist, who conducted weekly elk counts from a vehicle during crepuscular hours (generally 06: 00–10:00 and 17:00–19:00, 15% of surveys occurred outside of these times). Surveys were driven in a consistent direction (north to south) and constant speed (10 mph) along the same portion of paved roadway that afforded unobstructed views across 76 established survey points and >95% of the study area (Fig. 1). At each site, the observer recorded all elk within a ca. 50 m radius of the survey point. Given the relatively small size of the study population ($n = 93$) and frequency of surveys (weekly, year-round), the observer was able to determine the exact number of groups to expect on each survey and would end the survey once all groups had been located. Likewise, the small home range (6 km^2) with excellent visibility allowed the observer to monitor the locations of all previously counted groups so that none were double counted. Finally, to minimize detection bias introduced by poor visibility, we removed all surveys on days with heavy fog (< 4% of the data).

2.3.2. GPS telemetry

Between 2012 and 2018, 8 adult elk (3 males and 5 females, 10% of adult population) were chemically immobilized via dart gun and collared with a GPS transmitter (all animals were captured according to protocols approved by the National Park Service Institutional Animal Care and Use Committee and following established guidelines; Appendix A). Collars collected one location every three hours and were deployed for 3 to 31 months (mean = 17 ± 8 [SD] months; Appendix A).

2.3.3. Satellite remote sensing-based animal detections

We manually georeferenced the locations of individual elk and cattle (using 'BisQue'; (Kvilekval et al., 2010) identified within fenced cow pastures (Fig. 1) using archived, high-resolution satellite images (i.e., ≤ 50 cm panchromatic images from WorldView-2/3 and GeoEye-2 satellites; $n = 31$). Each image provided coverage of the entire study area and was collected from 2012 to 2017 at 10:00 or 14:00 local time. A trained observer followed a standardized protocol to classify each species (Fig. 2) and the same expert observer manually validated all entries. Note that pens that temporarily held cattle adjacent to ranch compounds were excluded from analysis. It was not possible to evaluate detectability from this archived dataset, but we minimized detection bias by limiting the analysis to grazed pastures (i.e., wildlands were excluded), which did not have vegetation present at a height or density that might obscure animals from above. In addition, there were no other large mammal species (e.g., black-tailed deer) detectable at this resolution. This resulted in the following distribution of seasonal population surveys across the study area: wet season ($n = 19$), parturition ($n = 3$), summer ($n = 1$), and mating season ($n = 8$).

2.3.4. Habitat characteristics

We obtained data on the spatial extent of habitat characteristics known to be important to the selection of habitat by elk (Cobb, 2010; Stewart et al., 2015). These features included: fenced cattle pastures, cattle density within fenced pastures, vegetation cover (e.g., percent cover for scrub, dry grassland, moist grassland, and heavily grazed grassland), distance to ponds, slope, aspect, and elevation ([dataset] Kinyon, 2015; Table 1). We then computed slope 'northness' (i.e., a proxy for solar radiation) as the cosine of aspect and used the mean Normalized Difference Vegetation Index (NDVI) for each season as an index of seasonal forage availability (computed using Landsat Tier 1 data accessed and processed via Google Earth Engine; Gorelick et al., 2017). We then masked land cover types that might confound NDVI

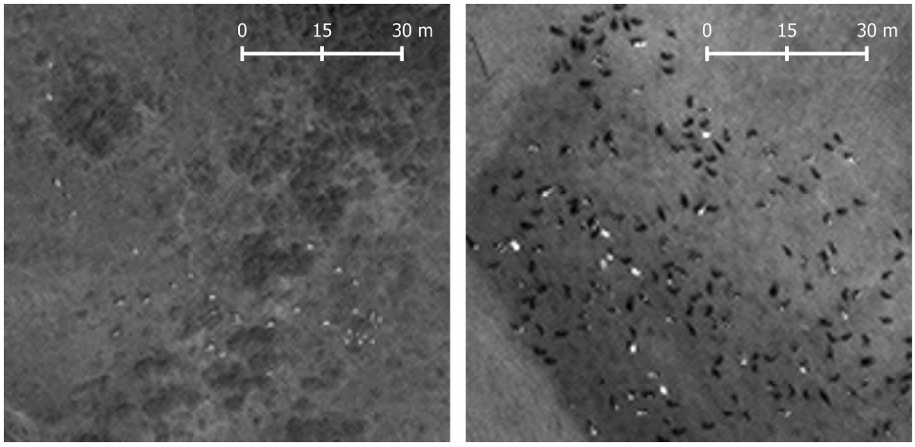

Fig. 2. Representative satellite images of elk (left) and cattle (right). Note that elk (smaller, lighter colored, generally lower density) and cows (larger, darker or multi-colored, generally higher density) differ with respect to size and color of individuals, as well as herd size. Examples shown are unprocessed panchromatic images, collected at 50 cm resolution (WorldView-2 satellite imagery © Maxar Technologies).

Table 1
Fixed effects included in the global model. The global model used visual survey and GPS collar datasets to quantify habitat selection for tule elk in the Drake's Beach herd at Point Reyes National Seashore 2010–2018. Random effects included: Elk ID, Site ID, and Year.

Category	Covariate	Definition	Unit	Cell size (m^2)	Mean	SD
Environment	Elevation	Height above sea level	Meters	100	51.4	23.2
	Northness	Relative measure of direction of slope face (i.e., cosine (aspect))	−1 to 1	100	0.0	0.6
	Ponds	Distance to nearest pond	Meters	100	407.5	271.3
	Slope	Slope of terrain	Degrees	100	18.0	12.7
Livestock	Cattle Density	Mean (non-zero)[a] density of cattle within cell during season of interest	Cows/ acre	100	–	–
	Pasture	Land within the boundaries of a ranch lease	% cover	100	80.1	37.8
Vegetation	Grassland: Dry	Vegetation type (e.g., *Baccharis* spp., *Lupinus* spp.)	% cover	100	55.2	43.4
	Grassland: Heavily Grazed	Highly disturbed vegetation due to agricultural activities (exclusive of silage or crop production)	% cover	100	17.1	35.6
	Grassland: Moist	Vegetation type (e.g., *Deschampsia* spp., *Carex* spp., *Juncus* spp.)	% cover	100	11.7	26.6
	NDVI	Median NDVI (Normalized Diference Vegetation Index) for season of interest	-1 to 1	900	–	–
	Scrub	Vegetation type (e.g., *Baccharis* spp., *Rhamnus* spp., *Toxicodendron* spp.)	% cover	100	22.0	35.7
Interactions	NDVI * Cattle Density	–	–	–	–	–
	NDVI * Moist Grassland	–	–	–	–	–
	NDVI * Scrub	–	–	–	–	–
	Slope * Cos Aspect	–	–	–	–	–

[a] Median density used for wet season models in all datasets.

calculations (i.e., water, beaches, dunes, and riparian vegetation) and rasterized all vector datasets to 10 m resolution ("raster" package; Hijmans, 2017). Seasonal cattle densities were estimated for fenced pastures (Fig. 1) by summarizing the SRS-based detections (see Section 2.3.3) as follows: (1) mean density per pasture; (2) median density per pasture; (3) mean density of non-zero counts per pasture; (4) median density of non-zero counts per pasture. Model selection was then used to determine the most appropriate 'cattle density' metric for each season (see Section 2.4.1).

2.4. Data analysis

2.4.1. Visual surveys

To address concerns about the independence of surveys conducted on the same day, we randomly rarefied the data to no more than one survey per day (thereby eliminating 18% of surveys). We then used the number of elk observed at each survey site per visit as our primary response variable. Mean covariate values (Table 1) within a 50-m radius buffer of each survey point served as covariates. We rescaled all quantitative covariates prior to analysis (by subtracting the mean from each input variable and dividing by two times its standard deviation; Gelman, 2008) and removed any with pairwise $r > 0.5$ or VIF > 3 (Zuur et al., 2009). As a result, streams were the only covariate removed from the analysis prior to model selection.

We modeled elk counts using a zero-altered (hurdle) negative binomial (ZANB) process model with a logit-link for the zero-prediction component and a log-link for the count-regression component ("glmmTMB" package; Magnusson et al., 2016; Zuur et al., 2009). The full ZANB model included the full set of environmental covariates and interactions in both the zero-prediction and count components. We modeled 'Year' and 'Site ID' as random-intercepts for both the zero-prediction and the count-regression components to account for potential sources of non-independence such as spatial clustering. We assessed goodness-of-fit for the full model by visually examining scaled (quantile) residuals and performing diagnostic tests (uniformity, overdispersion, zero-inflation, outliers) using the "DHARMa" package (Hartig, 2019).

For each season, we employed a two-step information-theoretic approach to model selection of habitats, in each instance selecting the lowest-AIC model (Burnham and Anderson, 2007): (1) We selected the best-performing estimate of cattle density from among the four candidate estimates (mean, median, mean non-zero, median non-zero; see Section 2.3.3), and (2) We then used backward stepwise selection ("buildmer" package; Voeten, 2019) based on AIC to remove any variables and interaction terms that were uninformative for both the zero-prediction and count-regression sub models. It should be noted that although these models necessarily treated observations as independent, the Drake's Beach Herd regularly moves as a single group, so confidence intervals on coefficients (and corresponding "significance") should be interpreted with caution.

2.4.2. GPS telemetry

We fitted seasonal Resource Selection Function (RSF) models using a generalized linear mixed modeling framework (GLMM) with a binomial error distribution and a logit-link. Available (background) points were randomly selected from within the 100% minimum convex polygon enclosing all known elk locations ($n = 5\times$ the total 'used' locations from telemetry). Covariate values (Table 1) were computed as the mean value within a 25 m radius of each 'used' or 'available' point (approximate scale of GPS error). We rescaled covariates and tested for collinearity as described for the visual survey analyses. Among-individual variation in habitat selection was modeled with random effects for all model coefficients (Gillies et al., 2006). Models were fitted using the "glmmTMB" package (Magnusson et al., 2016). Following Muff et al. (2019), we fixed the variance for the random intercept term at a high value and "infinitely" weighted used and available points. Finally, we used backward stepwise selection ("buildmer" package; Voeten, 2019) based on AIC to remove any uninformative variables and interaction terms. It should be noted that although these models necessarily treated individuals as independent, the Drake's Beach Herd regularly moves as a single group, so confidence intervals on coefficients (and corresponding "significance") should be interpreted with caution.

2.4.3. Satellite remote sensing-based animal detections

We first examined differences in the spatial distributions of georeferenced elk and cattle using a multi-response permutation procedure (MRPP; Talbert and Cade, 2013). This involved testing whether mean within-group Euclidean distances (i.e., cattle to cattle or elk to elk, aggregated across all 28 satellite images where elk were observed in cow pastures) were shorter than mean elk-cattle distances (Stewart et al., 2015). We report the average within-group pairwise distance (or delta value), which is a descriptive metric of spatial dispersion, and a p-value from the permutation procedure (fraction of permutation-based delta

values that are lower than the observed delta value; Oehlers et al., 2011; Stewart et al., 2015; Talbert and Cade, 2013). Since MRPP is not sensitive to spatial scale, delta values are a descriptive measure of spatial dispersion and we used them to establish a null model of group cohesion (Oehlers et al., 2011), as a preliminary step in the subsequent analysis.

To test whether observed differences in space-use by elk vs. cattle resulted from behavioral avoidance, we developed a bootstrap procedure to generate a distribution of elk locations under a null model (no cattle avoidance). To do this, we first aggregated all elk locations across all images where elk were visible inside of fenced pastures ($n = 28$) and constructed a kernel-density surface across our study site representing the probability of utilization by elk ("kde2d" function in the "MASS" package; Ripley et al., 2017). We then categorized elk into groups within each image (elk within 50 m of each other were considered part of the same group). Next, we used this kernel-density surface to generate hypothetical centroids for elk groups within each image (the number of simulated elk groups was held equal to the number observed in each image). For each image, we generated elk locations under the null model by sampling randomly from the observed distribution of location to group-centroid distances, holding the number of elk per group to observed values (directions from the group-centroid were generated randomly). For each bootstrap simulation replicate, we computed: (1) Mean distance from each simulated elk location to the nearest observed cattle location, averaged across all images ($n = 28$); (2) Minimum per-image distance from each simulated elk location to the nearest cattle location, averaged across all images; and (3) Proportion of elk groups occurring within 50 m of one or more cattle groups, averaged across all images. We compared the observed test statistics (e.g., mean distance from elk to nearest cattle location) with the distribution of each statistic generated under the null (no avoidance) model, and used this information to compute a *p*-value.

3. Results

3.1. Visual surveys

Visual surveys resulted in 1,792 observations of elk groups over 589 surveys (mean group size = 34, min = 10, max = 104; excluding zeros). The resource selection analysis conducted on the visual survey data indicated that, at the home range scale, all grazed cattle pastures were consistently avoided by elk (Figs. 3–5, Appendix B). Similarly, high cattle density had a consistently negative effect on selection by elk, regardless of season or NDVI value associated with cattle pastures (Figs. 3, 5, Appendix B).

Of the other environmental variables tested in our resource selection models, 'northness' (i.e., cos aspect) and elevation were consistently important for predicting selection of habitats by elk across all seasons except mating. Specifically, elk were more likely to be present in large numbers at high elevation sites and on south-facing slopes (Fig. 3, Appendix B). In addition, habitat near ponds was one of the most important

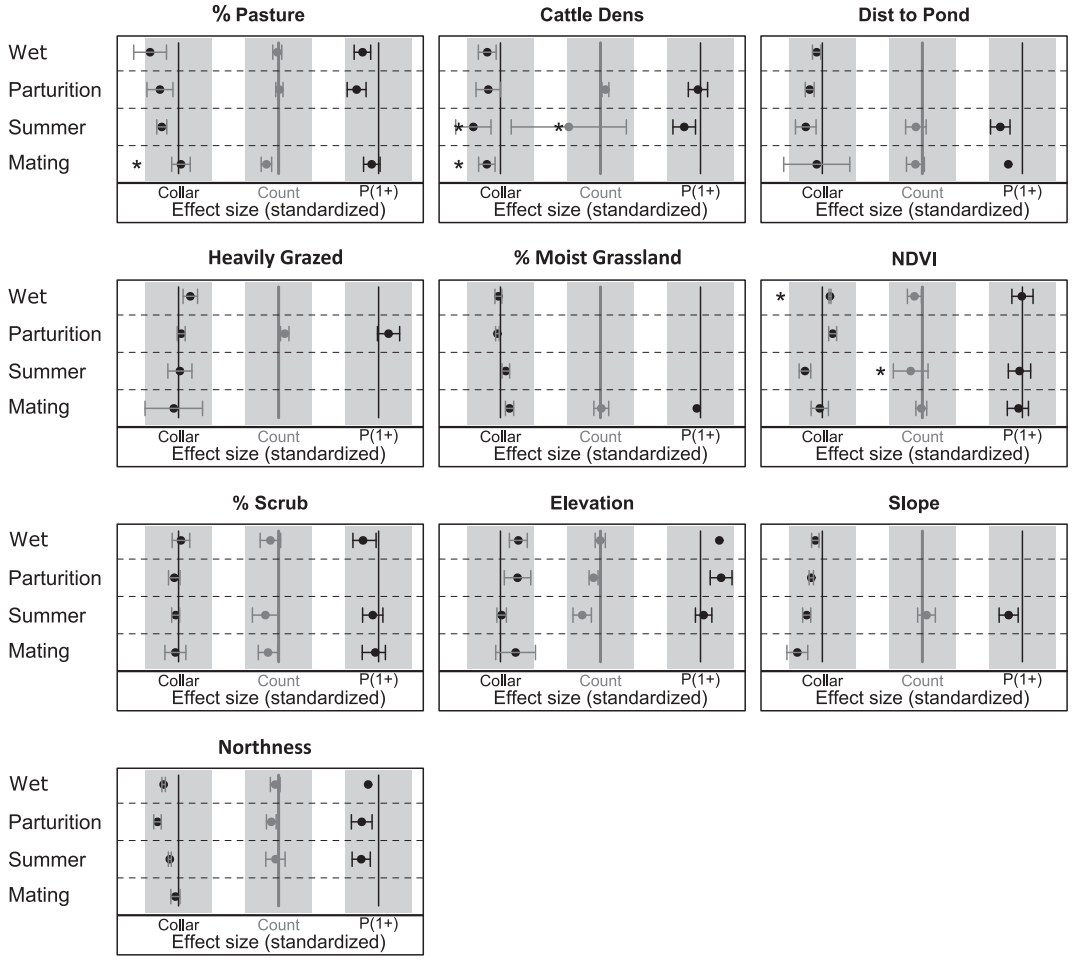

Fig. 3. Habitat selection coefficient estimates for tule elk at Point Reyes National Seashore. Coefficients were derived from GPS collar data (columns labeled 'Collar') and visual surveys (columns labeled 'Count' and 'P(1+)'), where 'P(1+)' represents probability of presence (one or more elk observed) and 'Count' represents expected elk abundance at occupied sites. Vertical lines indicate no effect, and gray regions represent standardized coefficient values between −2 and 2. Error bars represent 1 standard error (s.e). Asterisks denote that the estimated effect size and standard error was 5× larger in magnitude than what is depicted here (for visual clarity; see Appendix B for coefficient values).

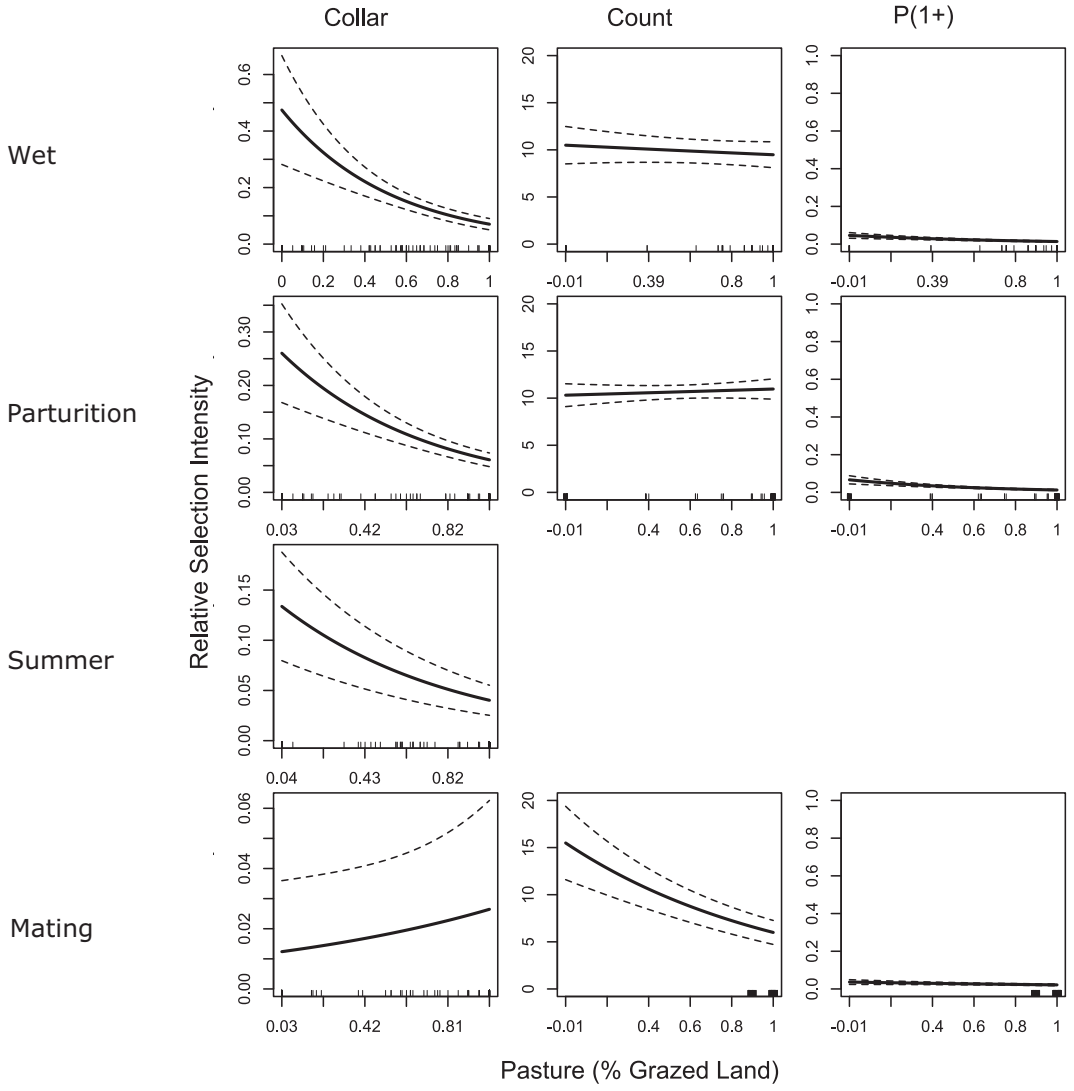

Fig. 4. Partial-dependence plots of elk habitat selection. Probability of habitat selection by elk as a function of the percentage of grazed land (Pasture) across multiple seasons and model types. Predictions were derived from GPS collar data ('Collar'; predictions represent point intensity) and visual survey data ('Count' and 'P(1+)'), where 'P(1+)' represents probability of presence (one or more elk observed) and 'Count' represents expected elk abundance at occupied sites. Blank panels denote that Pasture was not included in the top model for a particular season/model combination. Error bars represent 1 standard error (s.e).

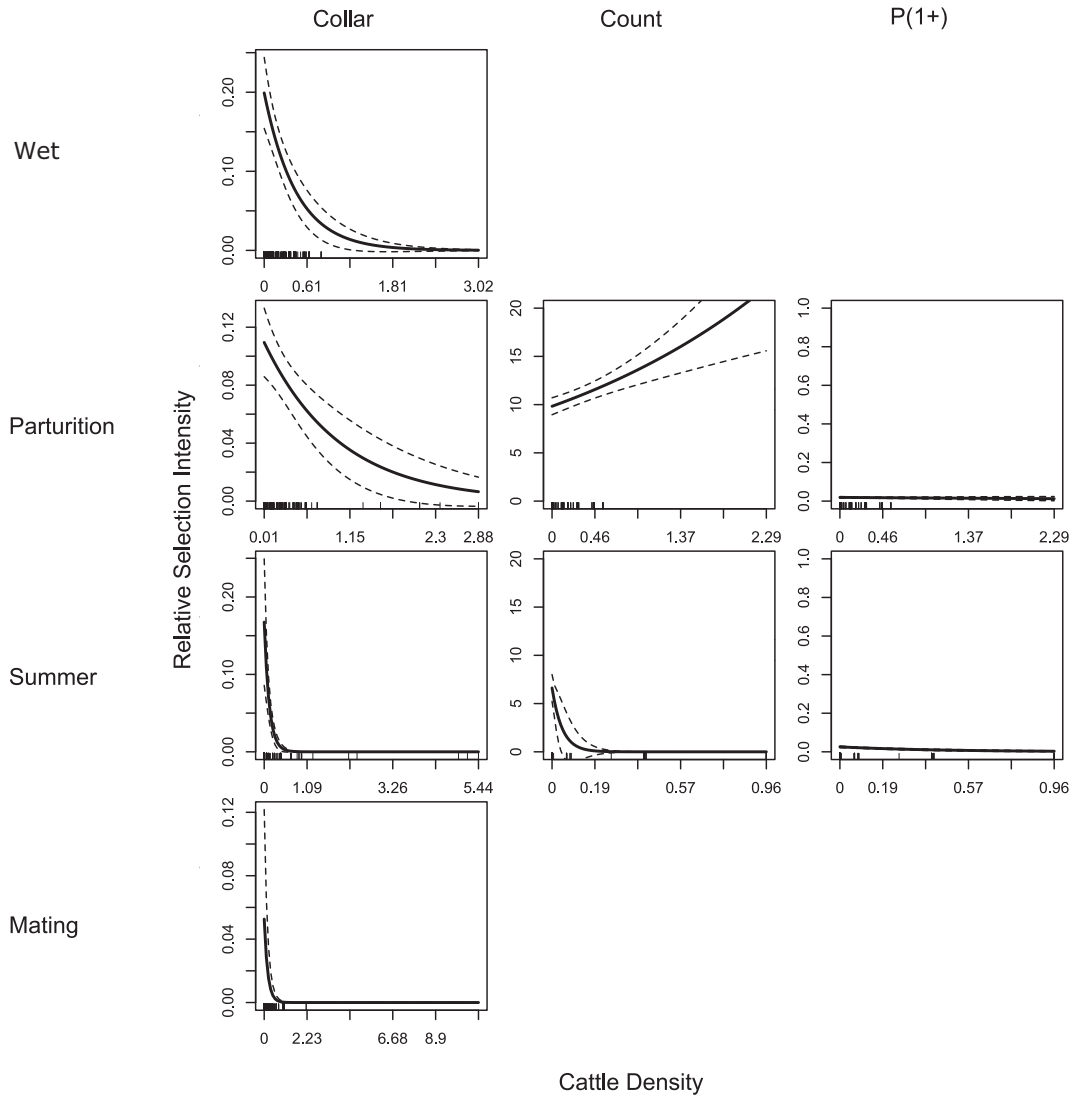

Fig. 5. Partial-dependence plots of elk habitat selection. Probability of habitat selection by elk as a function of cattle density across multiple seasons and model types. Predictions were derived from GPS collar data ('Collar'; predictions represent point intensity) and visual survey data ('Count' and 'P(1+)'), where 'P(1+)' represents probability of presence (one or more elk observed) and 'Count' represents expected elk abundance at occupied sites. Blank panels denote that Cattle Density was not included in the top model for a particular season/model combination. Error bars represent 1 standard error (s.e).

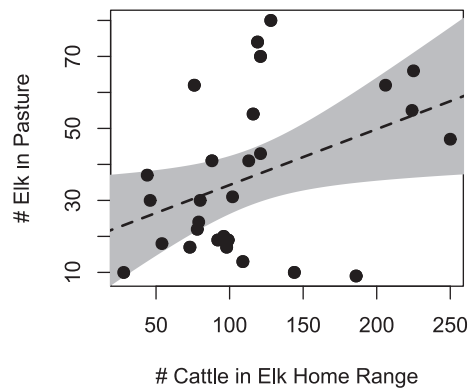

Fig. 6. Distribution of elk and cattle observed simultaneously in satellite images. Relationship between the number of elk observed in pastures at specific points in time (classified from satellite imagery; $n = 28$) and the corresponding total number of cattle observed within pasture areas commonly visited by elk (cattle occurring within the 95% kernel density contour for elk across all satellite images; $R^2 = 0.17$, adjusted $R^2 = 0.14$).

predictors of elk abundance for summer and mating seasons, while a gentle slope was an important predictor of elk abundance for summer only (Fig. 3, Appendix B). Grassland type (e.g., moist, dry, heavily grazed) was generally not an important predictor of elk abundance or presence for any season, although it was retained in the top models for parturition (heavily grazed only) and mating (moist grassland only). Both NDVI and scrub were retained in the top model for all seasons except parturition (Fig. 3, Appendix B).

For interactive effects, we found that, at high cattle densities, elk tended to avoid areas with high NDVI, whereas at low cattle densities elk tended to exhibit positive to neutral selection for NDVI (summer only; Appendix B). In addition, the relationship between elk presence and abundance with NDVI was always positive, but was generally weaker in areas of high scrub cover than low scrub cover (wet season only; Appendix B), as well as areas of high moist grass cover versus low moist grass cover (mating season only; Appendix B). Finally, at sites with gentle slopes, elk exhibited negative to neutral selection for north facing aspect (summer only; Appendix B).

3.2. GPS telemetry

GPS telemetry monitoring resulted in 29,014 fixes for 8 individuals (mean = 3,627, min = 594, max = 6,921 fixes/animal; mean fix success rate = 96%, min = 86%, max = 100%). The resource selection analysis conducted on this dataset indicated that, at the scale of the home range, all grazed cattle pastures were consistently avoided by elk (Figs. 3–5). Similarly, high cattle density had a consistently negative effect on selection by elk, regardless of season or NDVI value associated with cattle pastures (Figs. 3, 5, Appendix B). Of the remaining variables tested, 'northness' (i.e., cos aspect), elevation, and proximity to ponds were consistently important for predicting selection of habitats by elk across all seasons. Specifically, high elevation sites, south-facing slopes, and habitat near ponds were selected by elk (Fig. 3, Appendix B). Elk also generally selected for gentler slopes (Fig. 3, Appendix B). Although heavily grazed and moist grasslands were retained in top models across all seasons for this dataset, results showed strong selection for heavily grazed areas during the wet season only and moist grasslands during summer and mating seasons (Fig. 3, Appendix B). Dry grasslands were not retained in the top model for any season.

Selection along the NDVI gradient was seasonally variable, with selection for high NDVI sites during wet season and parturition, but avoidance of high NDVI sites during the summer (Fig. 3, Appendix B). As noted in Section 3.1, this pattern of avoidance was not corroborated by visual survey data, but a Wilcoxon Rank Sum analysis indicated that NDVI values were significantly lower outside of grazed pastures than inside and that this difference was most pronounced during the summer ($p < 0.001$, 95% CI [−0.125–0.115]; wet season: $p < 0.001$, 95% CI [−0.064–0.058]; parturition: $p < 0.001$, 95% CI [−0.029–0.022]; mating: $p < 0.001$, 95% CI [−0.021–0.009]). Elk also selected for high NDVI sites, regardless of moist grassland cover (Appendix B), but exhibited negative selection for NDVI at high scrub densities and positive selection for NDVI at lower scrub densities (except for the wet season when selection for NDVI was always positive; Appendix B). Finally, elk generally but weakly avoided scrub habitats across all seasons (Fig. 3, Appendix B) and selected for low slope areas, regardless of aspect or season (Appendix B).

3.3. Satellite remote sensing-based animal detections

The satellite image analysis resulted in 1,608 elk locations (mean = 51, min = 0, max = 98 elk, $n = 28$ images) and 26,943 cattle locations (mean = 869, min = 312, max = 1,251 cows, $n = 31$ images). Results from the multi-response permutation procedure indicated that the spatial distributions of elk and cattle within pasture areas were highly distinct and that cattle were more widely dispersed than elk ($\delta_{cattle} = 2{,}711$, $\delta_{elk} = 1{,}203$; $P < 0.0001$; Appendix C). Despite strong evidence for spatial segregation between elk and cattle, we did not observe behavioral avoidance of cattle by elk on the basis of satellite images; the observed distances between elk and cattle locations in any given image (total distance from each elk to nearest cow: mean = 516 m, min = 114 m, max = 1,433 m; minimum distance from each elk to nearest cow: mean = 361 m, min = 23 m, max = 1,378 m) did not significantly differ from a null model in which cattle locations had no effect on elk locations ($p = 0.28$ for mean distances and $p = 0.18$ for minimum distances; Appendix C). Individual cattle and elk, however, were never observed to come into direct contact and only 4% of observed elk groups overlapped with one or more cattle groups (overlap was defined as any individual elk occurring within 50 m of an individual cow), which was also consistent with a null model of no avoidance ($p = 0.31$; Appendix C). Furthermore, we detected a weakly positive relationship between elk use of pastures and the number of cattle occupying pasture areas commonly used by elk ($p = 0.03$, adjusted $R^2 = 0.13$, $n = 28$; Fig. 6), whereas a negative relationship might be expected under a cattle-avoidance hypothesis.

4. Discussion

Our study sought to explain patterns of habitat selection exhibited by a reintroduced population of elk that resides year-round in a rangeland shared with domestic cattle. By employing multiple, complementary data streams, we have identified patterns of habitat selection that vary across spatial scales but remain consistent over time. This approach revealed a more nuanced understanding of scale-dependent processes than would be possible from any single method and allowed the weaknesses of each dataset to be offset by the strengths of another. For example, location data from GPS collars and visual surveys revealed consistent patterns of habitat selection at the home range scale, while herd locations obtained from satellite images provided novel explanations for the patterns observed at both fine (< 100 m) and large (i.e., home range) spatial scales. Likewise, the low temporal resolution and large sample size of visual survey data was complemented by the high temporal resolution and limited sample size of the GPS collar data. These findings demonstrate the value of leveraging multiple methods for the study of habitat selection and highlight opportunities for the use of emerging satellite technologies to advance both basic and applied understanding of the rangeland-wildland interface.

Our analyses revealed that, at large scales, cattle-associated variables were the primary drivers of habitat selection by elk in this system, with elk occurrence being negatively associated with cattle density and cow pastures across all seasons. While it was not possible to fully disentangle

the effects of cattle presence from the effects of plant communities associated with cow pastures and wildlands (i.e., wildlands were dominated by native grassland while cow pastures were dominated by open coastal scrub), all vegetation variables we tested had a consistently smaller effect size than cattle density or proximity to pastures. Findings related to non-cattle variables were generally consistent with expectations for all species of North American elk (Thomas and Toweill, 2002), as well as previous studies of habitat selection by tule elk (Cobb, 2010; Huber et al., 2011). However, the degree to which cattle affected habitat selection by elk in this ecosystem was previously unknown and revealed unexpected relationships between cattle presence, vital resources, and habitat selection patterns of this once-imperiled native ungulate.

In temperate grasslands, NDVI typically serves as a reliable and positive predictor of habitat use by resident herbivores (Heffelfinger et al., 2020). While this relationship was evident for most seasons in our study, it was notably reversed during the summer, when NDVI values were significantly higher inside of cow pastures than in adjacent wildlands. As a result, we suspect that adult females with dependent young may have avoided cow pastures at the cost of grazing opportunities during this sensitive time of year. When combined with the patterns of avoidance documented at the home range scale, these observations strongly suggest that coexistence between cattle and elk is at least partially maintained by the tendency for elk to avoid cattle or cattle-associated habitats at large spatial scales. Although the limited sample size of this study prevented further exploration of sex-specific differences in resource selection, we present this finding to highlight the importance of considering this variable in future studies.

Despite the patterns of avoidance observed at large scales, we found little evidence for avoidance of cattle by elk at the pasture scale, which suggests that these species may exhibit an unusual tolerance for proximity at fine spatial scales (Stewart et al., 2002). While it is possible that this pattern was driven by a few bold individuals (i.e., $< 4\%$ of SRS-derived elk observations were within 50 m of cattle) or the uneven temporal sampling of the satellite data (i.e., 87% of images are from wet and mating seasons, which account for 66% of the observation period), similar cases of behavioral habituation between elk and cattle have been reported from other ecosystems where both species occur year-round on shared pastures (Yeo et al., 1993). In addition, we found a weak, but positive correlation between aggregate abundance of each species across the study area (Fig. 6). Taken together, these results imply that avoidance of cattle at the home range scale is not driven by behavioral intolerance, but by the need to partition shared resources at fine scales. Indeed, results from all three methods (e.g., GPS collars, visual surveys, satellite-based location data) supported this conclusion by confirming that elk consistently selected habitat in a manner that reduced the potential for forage competition with cattle, despite the occurrence of cattle across the majority (ca. 75%; Fig. 1 & Appendix C) of available grazing habitat.

While these conclusions have been drawn from an isolated population of elk in a limited geographic area, the behavioral mechanisms that support coexistence in this ecosystem (i.e., tolerance for proximity at small scales, but not at large scales) may have important implications for restoration projects elsewhere. For example, a cattle-dominated landscape with sufficient adjacent native habitat might warrant deeper consideration as a megafaunal reintroduction site than previously thought. However, we note that this tolerance for proximity could quickly become a liability for ecosystem managers if populations of wildlife or livestock increase or resources become limited due to extreme climatological shifts (i.e., drought or frost). As a result, the relationship between population size, climate, and reintroductions of non-migratory species at the rangeland-wildland interface will remain an important area of research moving forward.

In addition to informing the basic ecology of megafaunal reintroductions in non-migratory systems, this study provides a broadly applicable framework for advancing the study of species interactions through satellite remote sensing-based animal count data. Such information affords powerful opportunities to conduct cross-scale investigations of animal distributions and derive mechanistic explanations for observed patterns of habitat selection in a changing environment. For instance, these tools can facilitate studies of animal occurrence in response to an array of previously undetected environmental features, including spatially explicit distributions of conspecifics and heterospecifics, and the understudied role of microhabitats in resource selection by large wildlife (Hughey et al., 2018).

In the case of Point Reyes, satellite technology holds additional promise as a tool for the rapid assessment of disease risk in areas shared by elk and cattle. Specifically, the spread of 'Johne's disease' (*Mycobacterium avium paratuberculosis*) presents a unique opportunity to better understand how remote sensing might inform disease management in landscapes shared between elk and cattle. This incurable bacterial infection can be transmitted through ingestion of contaminated food or water and affects the small intestine of both wild and domestic ruminants, often with fatal consequences (Chiodini et al., 1984). While there is no public information on infection rates in cattle of Point Reyes, Johne's can persist in the environment for more than a year (Elliott et al., 2015) and has been documented in the study herd as recently as 2016 (Bernot and Press, 2018). As a result, it is important to continue to monitor changes in spatial overlap between the two species as part of a larger monitoring program, which includes additional testing and ground-based observations that account for site-specific interactions between contact rates, vaccine performance, host susceptibility, and the presence of other wildlife reservoirs (Gerritsmann et al., 2014; Knust et al., 2011).

While we caution that sufficient satellite coverage may not be feasible for many ecosystems (especially in forested or cloudy environments), a growing body of literature demonstrates the fresh promise of such methods for conducting large-scale biological monitoring in a variety of environmental contexts (e.g., LaRue et al., 2017) Pettorelli et al., 2014; Wang et al., 2019). Moreover, imminent advances in satellite imaging technology (e.g., increased spatiotemporal resolution, low-cost CubeSats, and democratization of AI technology) are rapidly reducing historic barriers to data access. Such developments will enhance our ability to study the ecology of open landscapes with precision and facilitate access to remote ecosystems around the world (Hughey et al., 2018; Weinstein, 2018).

5. Conclusions

Developing an in-depth understanding of how imperiled wildlife use the environments into which they have been reintroduced is a critical but often overlooked component of conservation. In this study, we evaluated the drivers of habitat selection by a native ungulate that was reintroduced to active rangelands defined by the year-round presence of cattle. We have used multiple, complementary data streams to reveal that cattle are the dominant drivers of habitat selection by reintroduced elk and that elk avoid cattle when possible (at large scales) and partition resources when necessary (at fine scales) in order to access limited grazing opportunities. Together, our three approaches have indicated the scale-dependent dynamics of habitat selection by a native ungulate and revealed new insights into elk-cattle interactions. In addition, contrary to common assumptions, our results indicate that native elk minimize their interactions with cattle and thus, in this ecosystem, grazing conflicts between wildlife and livestock may be limited.

Data availability statement

Code and data for all analyses presented in this paper are available on GitHub: https://github.com/kevintshoemaker/PRNS_Elk.

CRediT authorship contribution statement

Lacey Hughey: Conceptualization, Methodology, Formal Analysis, Data Curation, Writing- Original Draft, Review, & Editing, Visualization, Project Administration, Funding Acquisition. **Kevin Shoemaker**: Methodology, Software, Validation, Formal Analysis, Data Curation, Writing Original Draft, Review, & Editing, Visualization. **Kelley Stewart**: Methodology, Software, Formal Analysis, Writing Original Draft, Review, & Editing, Visualization. **Douglas McCauley**: Methodology, Writing- Review & Editing, Supervision, Funding Acquisition. **Hall Cushman**: Conceptualization, Writing- Review & Editing, Supervision, Project Administration, Funding Acquisition.

Declaration of competing interest

Lacey Hughey was an employee of Point Reyes National Seashore prior to development of this publication (2009–2014).

Acknowledgements

We thank David Press and Tim Bernot of Point Reyes National Seashore (NPS) for collection and management of all datasets. We also thank Dr. Benjamin Becker (NPS), Dr. Peter Gogan (USGS), and one anonymous reviewer for comments on early drafts of the manuscript. This work was supported by grants from the U. S. National Park Service, the National Science Foundation, and the DigitalGlobe Foundation.

Appendix A. Chemical immobilization and GPS collar deployment details

Table A1

Chemical immobilization details for elk captured during the study period. Seven animals were fitted with GPS collars from Advanced Telemetry Systems (GS110E/E2 Iridium, Minnesota, USA) and one (ID 24034B) was fitted with a Vectronics collar (Vertex Lite Iridium 2D GPS, Berlin, Germany). All animals were captured according to protocols approved by the National Park Service Institutional Animal Care and Use Committee (Protocol: PWR_PORE_PRESS_TULE_2012) and following established guidelines (Sikes and Animal Care and Use Committee of the American Society of Mammalogists, 2016).

Sex	Weight (kg)	2012 Immobilization	2012 Reversal	2013–2017 Immobilization	2013–2017 Reversal
Female	180	3 ml mixture of: 3 mg/kg Telazol 1.3 mg/kg xylazine	36 mg (3.6 ml 10 mg/ml yohimbine)	2.0 ml pre-mixed BAM: 54.6 mg butorphanol 18.2 mg azaperone 21.8 mg medetomidine	200 mg (1.0 ml 200 mg/ml tolazoline) 50 mg (1.0 ml 50 mg/ml naltrexone) 65 mg (2.6 ml 25 mg/ml atipamazole)
Male	250	4 ml mixture of: 3 mg/kg Telazol 1.3 mg/kg xylazine	50 mg (5.0 ml 10 mg/ml yohimbine)	3.0 ml pre-mixed BAM: 81.9 mg butorphanol 27.3 mg azaperone 32.7 mg medetomidine	200 mg (1.0 ml 200 mg/ml tolazoline) 50 mg (1.0 ml 50 mg/ml naltrexone) 100 mg (4.0 ml 25 mg/ml atipamazole)

References

Sikes, R.S., Animal Care and Use Committee of the American Society of Mammalogists, 2016. 2016 Guidelines of the American Society of Mammalogists for the use of wild mammals in research and education. J. Mammal. 97, 663–688. https://doi.org/10.1093/jmammal/gyw078

Table A2

Deployment schedule for all GPS collars used during the study period.

DEPLOYMENT 1

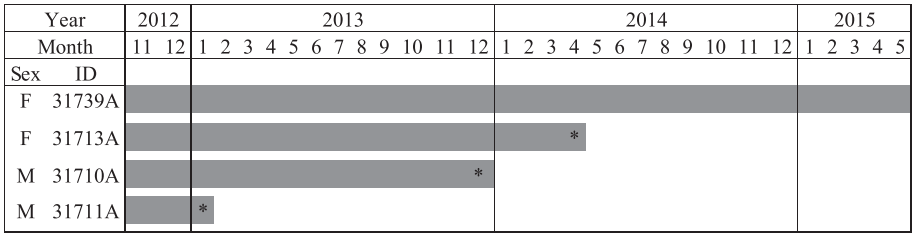

* Collar loss or failure

DEPLOYMENT 2

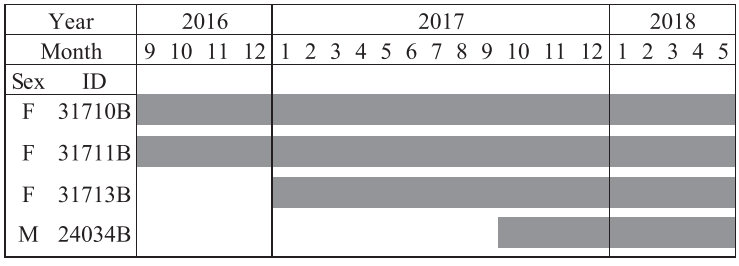

Appendix B. Coefficient values & interaction plots from Resource Selection Function analysis

Table B1

Summary values for all coefficients retained in top models. *Collar*: modeled from GPS collar data collected at Point Reyes National Seashore from November 2012 to March 2018 (see Appendix A for details). *Count and P(1+)*: Modeled from visual surveys conducted at Point Reyes National Seashore from September 2010 to November 2017. *Count* represents probability that elk abundance will increase as a function of each covariate. *P(1+)* represents probability of elk presence (one or more elk observed) as a function of each covariate.

		Collar		Count		P(1+)	
Variable	Season	Estimate	SE	Estimate	SE	Estimate	SE
Cattle Density	Mating	−4.08	1.48	NA	NA	NA	NA
Cos Aspect	Mating	−0.19	0.17	NA	NA	NA	NA
Dist to Pond	Mating	−0.34	1.19	−0.42	0.32	0.85	0.34
Elevation	Mating	0.91	0.72	NA	NA	NA	NA
High Intensity Ag	Mating	−0.29	1.04	NA	NA	NA	NA
Moist Grassland (%)	Mating	0.55	0.15	0.05	0.27	0.22	0.33
NDVI	Mating	−0.15	0.31	−0.07	0.2	0.23	0.36
NDVI*CattleDensity	Mating	NA	NA	NA	NA	NA	NA
NDVI*MoistGrass	Mating	−0.16	0.27	−1.35	0.41	0.28	0.58
NDVI*Scrub	Mating	−1.56	0.32	NA	NA	NA	NA
Pasture	Mating	0.72	1.68	−0.73	0.19	0.42	0.3
Scrub (%)	Mating	−0.19	0.38	−0.64	0.35	0.2	0.36
Slope	Mating	−1.5	0.38	NA	NA	NA	NA
Slope*CosAspect	Mating	−0.62	1.31	NA	NA	NA	NA
Cattle Density	Parturition	−0.73	0.44	0.3	0.12	0.15	0.35
Cos Aspect	Parturition	−1.26	0.14	−0.44	0.18	1.01	0.37
Dist to Pond	Parturition	−0.76	0.16	NA	NA	NA	NA
Elevation	Parturition	1.02	0.48	−0.42	0.16	−1.24	0.39
High Intensity Ag	Parturition	0.16	0.14	0.37	0.15	−0.6	0.4
Moist Grassland (%)	Parturition	−0.18	0.06	NA	NA	NA	NA
NDVI	Parturition	0.62	0.14	NA	NA	NA	NA
NDVI*CattleDensity	Parturition	NA	NA	NA	NA	NA	NA
NDVI*MoistGrass	Parturition	0.38	0.25	NA	NA	NA	NA
NDVI*Scrub	Parturition	−0.74	0.46	NA	NA	NA	NA
Pasture	Parturition	−1.12	0.47	0.05	0.13	1.32	0.34
Scrub (%)	Parturition	−0.26	0.21	NA	NA	NA	NA
Slope	Parturition	−0.66	0.08	NA	NA	NA	NA
Slope*CosAspect	Parturition	0.59	0.24	NA	NA	NA	NA
Cattle Density	Summer	NA	NA	NA	NA	NA	NA
Cos Aspect	Summer	−0.52	0.05	−0.19	0.35	1.04	0.33
Dist to Pond	Summer	−1	0.37	−0.39	0.37	1.33	0.35
Elevation	Summer	0.07	0.17	−1.1	0.33	−0.19	0.3
High Intensity Ag	Summer	0.08	0.43	NA	NA	NA	NA
Moist Grassland (%)	Summer	0.32	0.14	NA	NA	NA	NA
NDVI	Summer	−1.04	0.21	−3.51	3.13	0.17	0.4
NDVI*CattleDensity	Summer	−3.71	0.49	−15.1	14.16	1.27	0.91
NDVI*MoistGrass	Summer	0.13	0.16	NA	NA	NA	NA
NDVI*Scrub	Summer	−0.96	0.13	NA	NA	NA	NA
Pasture	Summer	−1.01	0.18	NA	NA	NA	NA
Scrub (%)	Summer	−0.17	0.14	−0.79	0.47	0.35	0.37
Slope	Summer	−0.94	0.15	0.25	0.32	0.83	0.34
Slope*CosAspect	Summer	0.4	0.35	2.42	0.9	1.15	0.68
Cattle Density	Wet	−0.79	0.32	NA	NA	NA	NA
Cos Aspect	Wet	−0.9	0.06	−0.2	0.18	0.63	0.27
Dist to Pond	Wet	−0.34	0.15	NA	NA	NA	NA
Elevation	Wet	1.07	0.32	−0.01	0.18	−1.13	0.29
High Intensity Ag	Wet	0.71	0.26	NA	NA	NA	NA
Moist Grassland (%)	Wet	−0.12	0.12	NA	NA	NA	NA
NDVI	Wet	2.28	0.18	−0.48	0.25	0.03	0.41
NDVI*CattleDensity	Wet	NA	NA	NA	NA	NA	NA
NDVI*MoistGrass	Wet	−0.21	0.18	NA	NA	NA	NA
NDVI*Scrub	Wet	0.53	0.17	−0.46	0.84	2.8	1.2
Pasture	Wet	−1.71	0.59	−0.08	0.16	0.96	0.29
Scrub (%)	Wet	0.14	0.32	−0.49	0.37	0.93	0.47
Slope	Wet	−0.42	0.13	NA	NA	NA	NA
Slope*CosAspect	Wet	−0.01	0.21	NA	NA	NA	NA

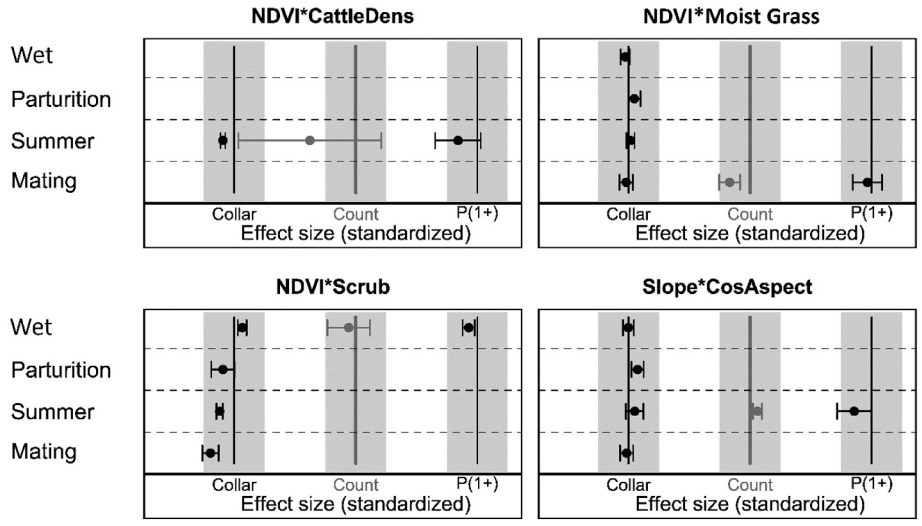

Fig. B1. Interactions between covariates related to patterns of habitat selection by tule elk. Vertical lines indicate an effect size of zero, and gray regions represent (standardized) effect sizes between −2 and 2. *Collar*: modeled from GPS collar data collected at Point Reyes National Seashore from November 2012 to March 2018 (see Appendix A for details). *Count and P(1+)*: Modeled from visual surveys conducted at Point Reyes National Seashore from September 2010 to November 2017. *Count* represents probability that elk abundance will increase as a function of each covariate. *P(1+)* represents probability of elk presence (one or more elk observed) as a function of each covariate. Error bars represent 1 standard error (s.e).

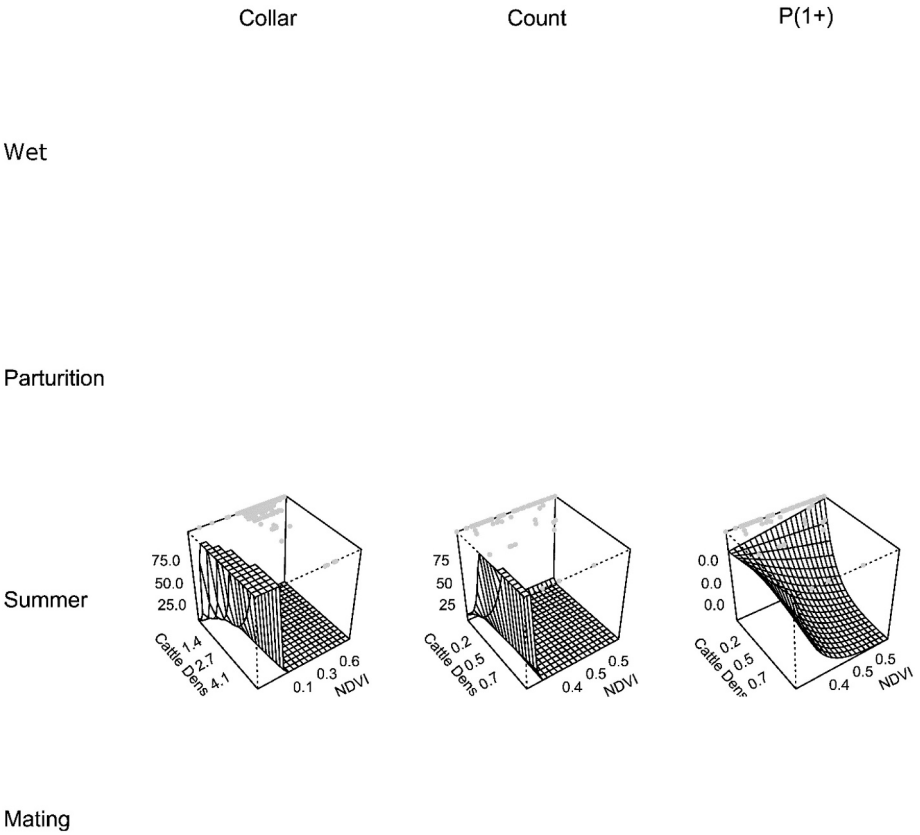

Fig. B2. Interaction between cattle density (Cattle Dens) and NDVI for predicting elk habitat selection. *Collar*: modeled from GPS collar data collected at Point Reyes National Seashore from November 2012 to March 2018 (see Appendix A for details); y axis represents selection intensity. *Count and P(1+)*: Modeled from visual surveys conducted at Point Reyes National Seashore from September 2010 to November 2017. *Count* represents probability that elk abundance will increase as a function of each covariate; y axis represents density at a survey point. *P(1+)* represents probability of elk presence (one or more elk observed) as a function of each covariate; y axis represents the probability of observing one or more elk at a survey point. Gray dots represent raw data, which is clustered at high NDVI values and low cattle densities. As a result, the apparent relationship between low cattle densities and low NDVI should be interpreted with caution. Blank panels denote that this interaction was not included in the top model for a particular season/model combination.

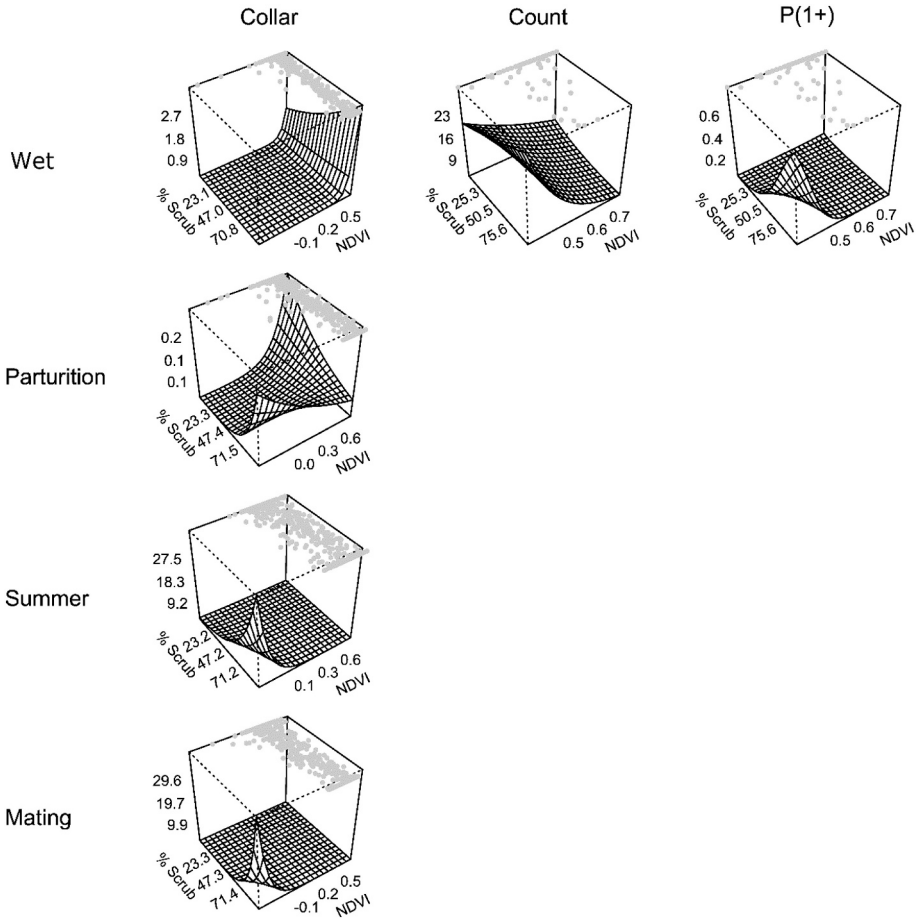

Fig. B3. Interaction between scrub vegetation and NDVI for predicting elk habitat selection. *Collar*: modeled from GPS collar data collected at Point Reyes National Seashore from November 2012 to March 2018 (see Appendix A for details); y axis represents selection intensity. *Count and P(1+)*: Modeled from visual surveys conducted at Point Reyes National Seashore from September 2010 to November 2017. *Count* represents probability that elk abundance will increase as a function of each covariate; y axis represents density at a survey point. *P(1+)* represents probability of elk presence (one or more elk observed) as a function of each covariate; y axis represents the probability of observing one or more elk at a survey point. Gray dots represent raw data and blank panels denote that this interaction was not included in the top model for a particular season/model combination.

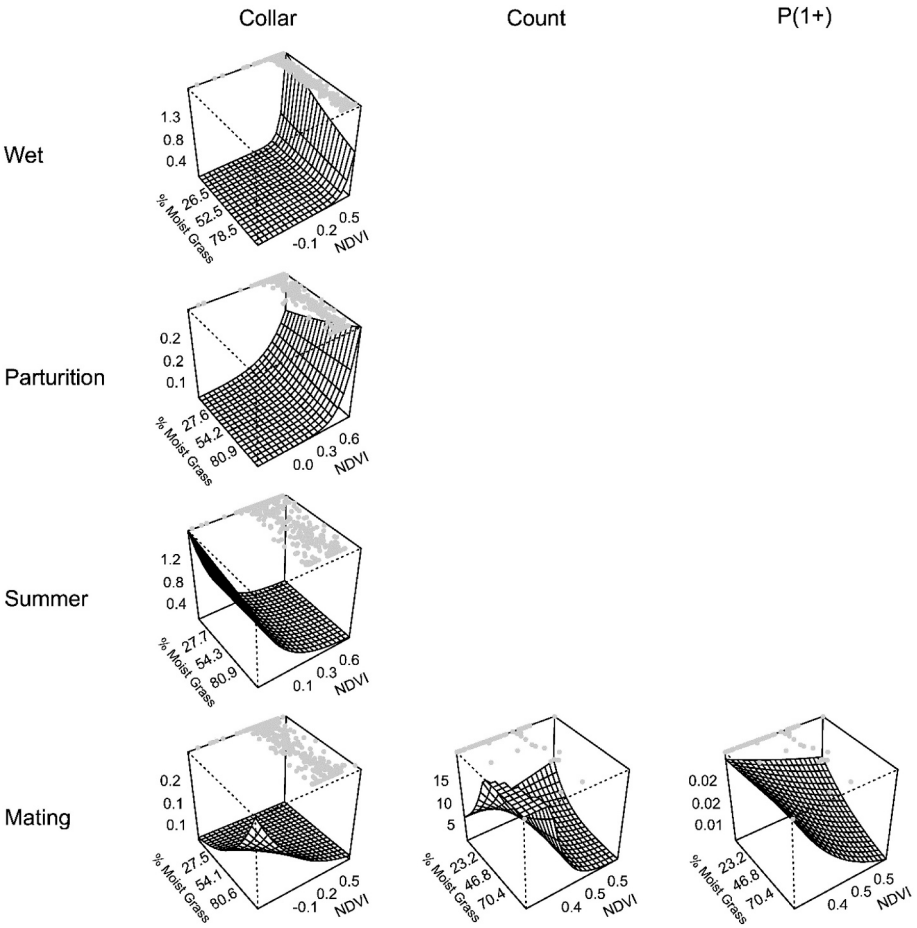

Fig. B4. Interaction between moist grasslands and NDVI for predicting elk habitat selection. *Collar*: modeled from GPS collar data collected at Point Reyes National Seashore from November 2012 to March 2018 (see Appendix A for details); y axis represents selection intensity. *Count and P(1+)*: Modeled from visual surveys conducted at Point Reyes National Seashore from September 2010 to November 2017. *Count* represents probability that elk abundance will increase as a function of each covariate; y axis represents density at a survey point. *P(1+)* represents probability of elk presence (one or more elk observed) as a function of each covariate; y axis represents the probability of observing one or more elk at a survey point. Gray dots represent raw data and blank panels denote that this interaction was not included in the top model for a particular season/model combination.

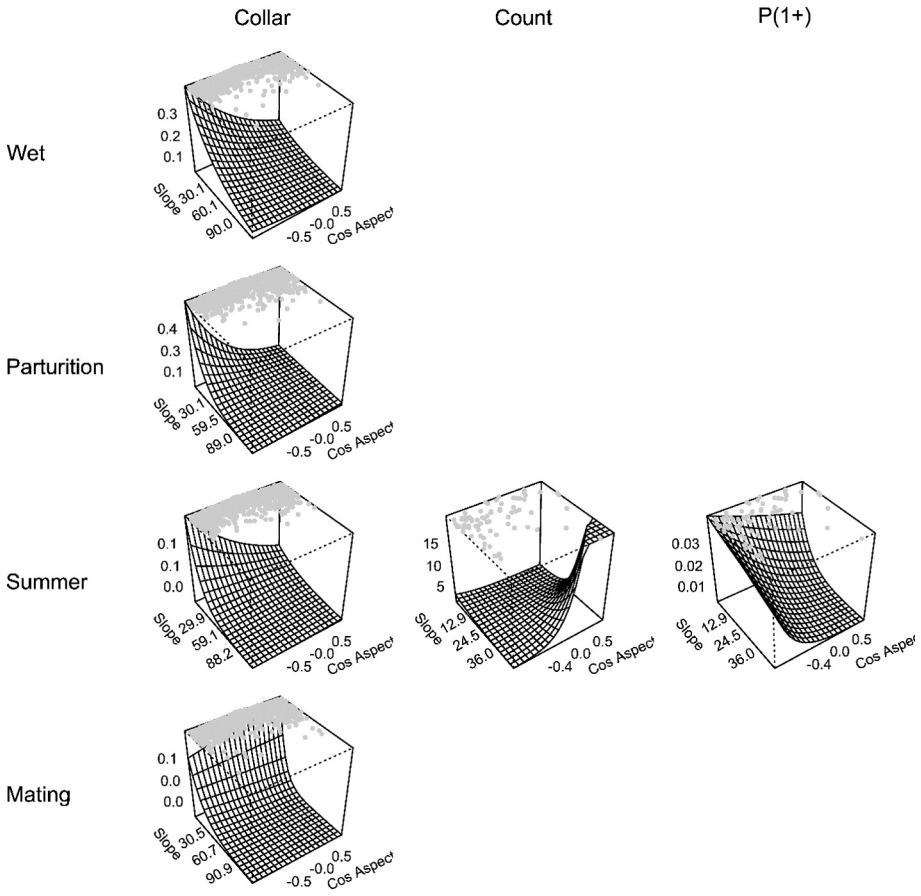

Fig. B5. Interaction between slope and 'northness' (cos aspect) for predicting elk habitat selection. *Collar*: modeled from GPS collar data collected at Point Reyes National Seashore from November 2012 to March 2018 (see Appendix A for details); y axis represents selection intensity. *Count and P(1+)*: Modeled from visual surveys conducted at Point Reyes National Seashore from September 2010 to November 2017. *Count* represents probability that elk abundance will increase as a function of each covariate; y axis represents density at a survey point. *P(1+)* represents probability of elk presence (one or more elk observed) as a function of each covariate; y axis represents the probability of observing one or more elk at a survey point. Gray dots represent raw data and blank panels denote that this interaction was not included in the top model for a particular season/model combination.

Appendix C. Satellite remote sensing-based species detections

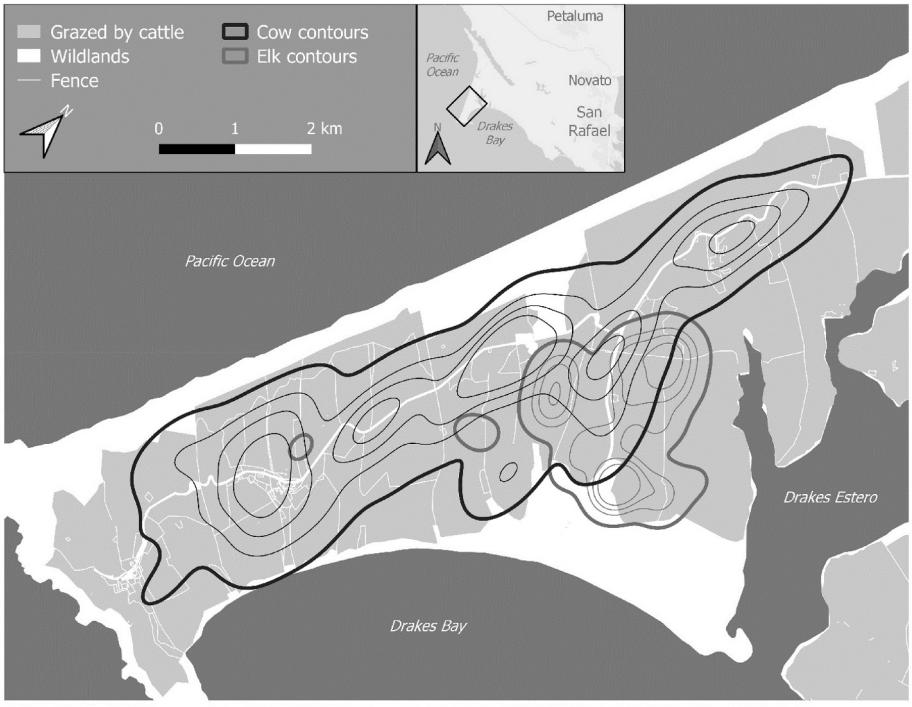

Fig. C1. Range overlap between elk and cattle within grazed pastures. Contours were created from satellite remote sensing-based animal detections (within grazed pastures only) and represent kernel density isopleths (95% contours bolded) for elk and cattle ($n = 28$, images from 2014 to 2018).

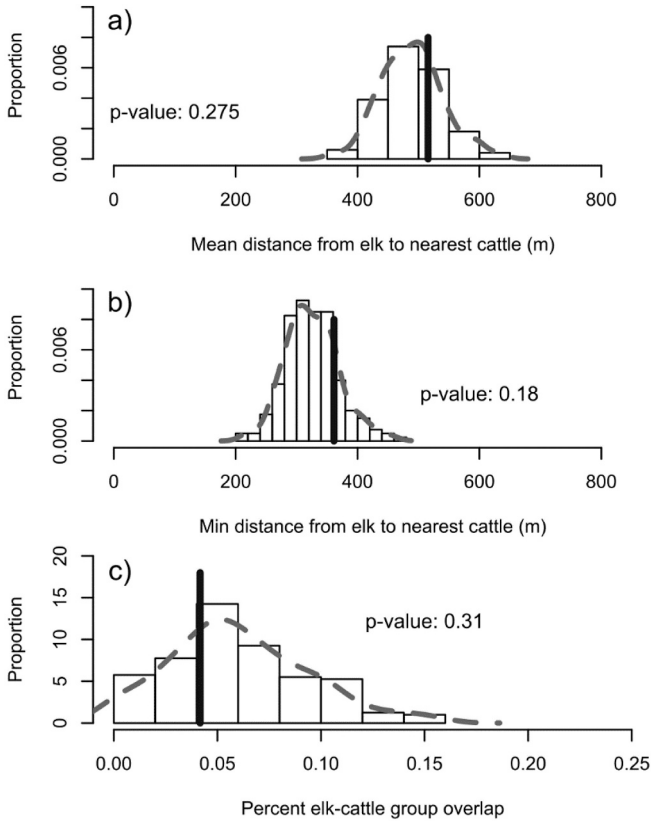

Fig. C2. Semi-parametric bootstrap tests of elk and cattle distributions obtained from satellite images. Observed metrics of elk-cattle spatial separation (thick vertical black lines) and the null distributions of these metrics (histograms; assuming elk locations were unrelated to cattle locations) are presented. Panels depict (a) mean distances from each randomly sampled elk location to the nearest cattle location, averaged across images; (b) minimum elk-cattle distances averaged across images; (c) the proportion of elk-cattle co-occurrences (defined as the fraction of elk groups for which any members were within 50 m of a cattle location), averaged across all images ($n = 28$).

References

Armstrong, D.P., Seddon, P.J., 2008. Directions in reintroduction biology. Trends Ecol. Evol. 23, 20–25. https://doi.org/10.1016/j.tree.2007.10.003.

Bernot, T., Press, D., 2018. Tule Elk Monitoring and Management at Point Reyes National Seashore: 2015–2016 Report (No. Natural Resource Report NPS/SFAN/NRR—2018/1656). National Park Service.

Burnham, K.P., Anderson, D.R., 2007. Model Selection and Multimodel Inference: A Practical Information-Theoretic Approach. Springer Science & Business Media.

Chave, J., 2013. The problem of pattern and scale in ecology: what have we learned in 20 years? Ecol. Lett. 16 (Suppl. 1), 4–16. https://doi.org/10.1111/ele.12048.

Chiodini, R.J., Van Kruiningen, H.J., Merkal, R.S., Others, 1984. Ruminant paratuberculosis (Johne's disease): the current status and future prospects. Cornell Vet. 74, 218–262.

Cobb, M.A., 2010. Spatial ecology and population dynamics of tule elk (*Cervus elaphus nannodes*) at Point Reyes National Seashore, California. Unpublished dissertation.

Elliott, G.N., Hough, R.L., Avery, L.M., Maltin, C.A., Campbell, C.D., 2015. Environmental risk factors in the incidence of Johne's disease. Crit. Rev. Microbiol. 41, 488–507. https://doi.org/10.3109/1040841X.2013.867830.

Fleming, C.H., Calabrese, J.M., 2016. A new kernel-density estimator for accurate home-range and species-range area estimation. Methods in Ecology and Evolution 8 (5), 571–579. https://doi.org/10.1111/2041-210X.12673.

Gelman, A., 2008. Scaling regression inputs by dividing by two standard deviations. Stat. Med. 27, 2865–2873. https://doi.org/10.1002/sim.3107.

Gerritsmann, H., Stalder, G.L., Spergser, J., Hoelzl, F., Deutz, A., Kuebber-Heiss, A., Walzer, C., Smith, S., 2014. Multiple strain infections and high genotypic diversity among Mycobacterium avium subsp. paratuberculosis field isolates from diseased wild and domestic ruminant species in the eastern Alpine region of Austria. Infect. Genet. Evol. https://doi.org/10.1016/j.meegid.2013.11.009.

Gillies, C.S., Hebblewhite, M., Nielsen, S.E., Krawchuk, M.A., Aldridge, C.L., Frair, J.L., Saher, D.J., Stevens, C.E., Jerde, C.L., 2006. Application of random effects to the study of resource selection by animals. J. Anim. Ecol. 75, 887–898. doi:https://doi.org/10.1111/j.1365-2656.2006.01106.x.

Gorelick, N., Hancher, M., Dixon, M., Ilyushchenko, S., Thau, D., Moore, R., 2017. Google earth engine: planetary-scale geospatial analysis for everyone. Remote Sens. Environ. 202, 18–27. https://doi.org/10.1016/j.rse.2017.06.031.

Hartig, F., 2019. DHARMa: Residual Diagnostics for Hierarchical (Multi-Level/Mixed) Regression Models. R Package Version 0.2.2.

Heffelfinger, L.J., Stewart, K.M., Shoemaker, K.T., Darby, N.W., Bleich, V.C., 2020. Balancing current and future reproductive investment: variation in resource selection during stages of reproduction in a long-lived herbivore. Front. Ecol. Evol. 8, 163.

Hibert, F., Calenge, C., Fritz, H., Maillard, D., Bouché, P., Ipavec, A., Convers, A., Ombredane, D., de Visscher, M.-N., 2010. Spatial avoidance of invading pastoral cattle by wild ungulates: insights from using point process statistics. Biodivers. Conserv. 19, 2003–2024. https://doi.org/10.1007/s10531-010-9822-0.

Hijmans, R.J., 2017. raster: Geographic Data Analysis and Modeling. R Package Version 2.8–19.

Howell, J.A., Brooks, G.C., Semenoff-Irving, M., Greene, C., 2002. Population dynamics of tule elk at point Reyes National Seashore, California. J. Wildl. Manag. 66, 478–490. https://doi.org/10.2307/3803181.

Huber, P.R., Greco, S.E., Hobbs, J., 2011. Assessment of habitat for the potential reintroduction of tule elk to the San Joaquin Valley, California. Calif. Fish Game 97, 117–129.

Hughey, L.F., Hein, A.M., Strandburg-Peshkin, A., Jensen, F.H., 2018. Challenges and solutions for studying collective animal behaviour in the wild. Philos. Trans. R. Soc. Lond. Ser. B Biol. Sci. 373 https://doi.org/10.1098/rstb.2017.0005.

Kinyon, J., 2015. Point Reyes National Seashore GIS Database.

Knust, B.M., Wolf, P.C., Wells, S.J., 2011. Characterization of the risk of deer-cattle interactions in Minnesota by use of an on-farm environmental assessment tool. Am. J. Vet. Res. 72, 924–931. https://doi.org/10.2460/ajvr.72.7.924.

Kvilekval, K., Fedorov, D., Obara, B., Singh, A., Manjunath, B.S., 2010. Bisque: a platform for bioimage analysis and management. Bioinformatics 26 (4), 544–552. https://doi.org/10.1093/bioinformatics/btp699.

LaRue, M.A., Stapleton, S., Anderson, M., 2017. Feasibility of using high-resolution satellite imagery to assess vertebrate wildlife populations. Conservation Biology 31 (1), 213–220. https://doi.org/10.1111/cobi.12809.

Magnusson, A., Skaug, H., Nielsen, A., Berg, C., Kristensen, K., Maechler, M., van Bentham, K., Bolker, B., Brooks, M., 2016. glmmTMB: Generalized Linear Mixed Models using Template Model Builder. R package version 0.02.

Merkle, J.A., Cross, P.C., Scurlock, B.M., Cole, E.K., Courtemanch, A.B., Dewey, S.R., Kauffman, M.J., 2018. Linking spring phenology with mechanistic models of host

movement to predict disease transmission risk. J. Appl. Ecol. 55, 810–819. https://doi.org/10.1111/1365-2664.13022.
Muff, S., Signer, J., Fieberg, J., 2019. Accounting for individual-specific variation in habitat-selection studies: efficient estimation of mixed-effects models using Bayesian or frequentist computation. J. Anim. Ecol. https://doi.org/10.1111/1365-2656.13087.
Oehlers, S.A., Bowyer, R.T., Huettmann, F., Person, D.K., Kessler, W.B., 2011. Sex and scale: implications for habitat selection by Alaskan moose *Alces alces gigas*. Wildlife Biol. 17, 67–84. https://doi.org/10.2981/10-039.
Pettorelli, N., Laurance, W.F., O'Brien, T.G., Wegmann, M., Nagendra, H., Turner, W., 2014. Satellite remote sensing for applied ecologists: opportunities and challenges. J. Appl. Ecol. https://doi.org/10.1111/1365-2664.12261.
Proffitt, K.M., Gude, J.A., Hamlin, K.L., Garrott, R.A., Cunningham, J.A., Grigg, J.L., 2011. Elk distribution and spatial overlap with livestock during the brucellosis transmission risk period. J. Appl. Ecol. 48, 471–478.
Ripley, B., Bates, D.M., Hornik, K., Gebhardt, A., Firth, D., 2017. MASS: functions and datasets to support venables and ripley, "Modern Applied Atatistics with S" (2002). R package version 7, 3–47.
Scasta, J.D., Beck, J.L., Angwin, C.J., 2016. Meta-analysis of diet composition and potential conflict of wild horses with livestock and wild ungulates on western rangelands of North America. Rangeland Ecol. Manage. 69, 310–318. https://doi.org/10.1016/j.rama.2016.01.001.
Schieltz, J.M., Rubenstein, D.I., 2016. Evidence based review: positive versus negative effects of livestock grazing on wildlife. What do we really know? Environ. Res. Lett. 11, 113003 https://doi.org/10.1088/1748-9326/11/11/113003.
Seddon, P.J., Griffiths, C.J., Soorae, P.S., Armstrong, D.P., 2014. Reversing defaunation: restoring species in a changing world. Science 345, 406–412. https://doi.org/10.1126/science.1251818.
Stewart, K.M., Bowyer, R.T., Kie, J.G., Cimon, N.J., Johnson, B.K., 2002. Temporospatial distributions of elk, mule deer, and cattle: resource partitioning and competitive displacement. J. Mammal. 83, 229–244. https://doi.org/10.1644/1545-1542(2002)083<0229:TDOEMD>2.0.CO;2.
Stewart, K.M., Walsh, D.R., Kie, J.G., Dick, B.L., Bowyer, R.T., 2015. Sexual segregation in North American elk: the role of density dependence. Ecol. Evol. 5, 709–721. https://doi.org/10.1002/ece3.1397.
Talbert, M.K., Cade, B.S., 2013. USGS open-file report 2005–1353: User manual for blossom statistical package for R [WWW document]. In: U.S. Geological Survey (USGS). URL. http://pubs.usgs.gov/of/2005/1353. (Accessed 18 June 2019).
Thomas, J.W., Toweill, D.E., 2002. North American Elk: Ecology and Management. Smithsonian Institution Press, Washington.
Voeten, C.C., 2019. Buildmer: Stepwise Elimination and Term Reordering for Mixed-effects Regression. R Package Version 1.1.
Wang, D., Shao, Q., Yue, H., 2019. Surveying wild animals from satellites, manned aircraft and unmanned aerial systems (UASs): a review. Remote Sensing. https://doi.org/10.3390/rs11111308.
Weinstein, B.G., 2018. A computer vision for animal ecology. J. Anim. Ecol. 87, 533–545. https://doi.org/10.1111/1365-2656.12780.
Western Regional Climate Center [WWW Document], 2020. Point Reyes RCA California climatological data summaries. URL. https://wrcc.dri.edu/cgi-bin/rawMAIN.pl?nvprca. (Accessed 10 January 2020).
Yeo, J.J., Peek, J.M., Wittinger, W.T., Kvale, Craig T., 1993. Influence of rest-rotation cattle grazing on mule deer and elk habitat use in east-Central Idaho. J. Range Manag. 46, 245–250. https://doi.org/10.2307/4002615.
Zuur, A., Ieno, E.N., Walker, N., Saveliev, A.A., Smith, G.M., 2009. Mixed Effects Models and Extensions in Ecology with R. Springer Science & Business Media.